

Sulfuric acid speleogenesis (SAS) close to the water table: Examples from southern France, Austria, and Sicily



Jo De Waele^{a,*}, Philippe Audra^b, Giuliana Madonia^c, Marco Vattano^c, Lukas Plan^d, Ilenia M. D'Angeli^a, Jean-Yves Bigot^b, Jean-Claude Nobécourt^e

^a Istituto Italiano di Speleologia, Dipartimento di Scienze Biologiche, Geologiche e Ambientali, University of Bologna, Via Zamboni 67, 40127 Bologna, Italy

^b University of Nice Sophia-Antipolis, CNRS, IRD, Observatoire de la Côte d'Azur, Geoazur UMR 7329 & Polytech Nice-Sophia, 930 route des Colles, 06903 Sophia-Antipolis, Nice, France

^c Dipartimento di Scienze della Terra e del Mare, University of Palermo, Via Archirafi 22, 90123 Palermo, Italy

^d Natural History Museum Vienna, Karst and Cave Working Group, Museumsplatz 1/10, 1070, Vienna, Austria

^e Crespe, 06140 Vence, France

ARTICLE INFO

Article history:

Received 22 April 2015

Received in revised form 23 October 2015

Accepted 25 October 2015

Available online 26 October 2015

Keywords:

Sulfuric acid caves

Hypogenic karst

Cave morphology

Speleogenesis

Condensation–corrosion

ABSTRACT

Caves formed by rising sulfuric waters have been described from all over the world in a wide variety of climate settings, from arid regions to mid-latitude and alpine areas. H₂S is generally formed at depth by reduction of sulfates in the presence of hydrocarbons and is transported in solution through the deep aquifers. In tectonically disturbed areas major fractures eventually allow these H₂S-bearing fluids to rise to the surface where oxidation processes can become active producing sulfuric acid. This extremely strong acid reacts with the carbonate bedrock creating caves, some of which are among the largest and most spectacular in the world. Production of sulfuric acid mostly occurs at or close to the water table but also in subaerial conditions in moisture films and droplets in the cave environment. These caves are generated at or immediately above the water table, where condensation–corrosion processes are dominant, creating a set of characteristic meso- and micromorphologies. Due to their close connection to the base level, these caves can also precisely record past hydrological and geomorphological settings. Certain authigenic cave minerals, produced during the sulfuric acid speleogenesis (SAS) phase, allow determination of the exact timing of speleogenesis. This paper deals with the morphological, geochemical and mineralogical description of four very typical sulfuric acid water table caves in Europe: the Grotte du Chat in the southern French Alps, the Acqua Fitusa Cave in Sicily (Italy), and the Bad Deutsch Altenburg and Kraushöhle caves in Austria.

© 2015 Elsevier B.V. All rights reserved.

1. Introduction

A constantly increasing number of caves are being classified as hypogenic caves since their clear distinction occurred only a few years ago (Klimchouk, 2007, 2009). These caves are typically formed by rising fluids which attain their aggressiveness from deep sources and not from the surface water containing CO₂. Sulfuric acid caves (SAS caves) are the most interesting and best studied among these (e.g. Egemeier, 1981; Hill, 1987; Galdenzi and Menichetti, 1995; Polyak et al., 1998; Hose and Pisarowicz, 1999; Audra, 2008; Palmer, 2013). They have been described for more than a century in Europe (e.g., Socquet, 1801; Hauer, 1885; Principi, 1931; Martel, 1935). Speleogenetic studies were carried out first in American caves (Morehouse, 1968), while the earliest

sulfuric acid speleogenesis (SAS) model was published by Egemeier (1981), relying on observations in Lower Kane Cave in Wyoming (USA).

An increasingly larger number of SAS caves are known around the world, and an overview of these is given in Table 1.

The voids in SAS caves are mostly formed above the water table by abiotic and/or biotic oxidation of H₂S deriving from a deep source (Galdenzi and Maruoka, 2003; Jones et al., 2014, 2015). H₂S can derive from volcanic activity, reduction of sulfates, such as gypsum or anhydrite, or hydrocarbons and is brought to the surface through deep tectonic structures. The origin of sulfur and its possible sources can usually be deciphered using the stable isotope signature of sulfur (Onac et al., 2011). Oxidation of H₂S produces sulfuric acid that reacts instantaneously with the carbonate host rock producing replacement gypsum and carbon dioxide. CO₂ can dissolve in water and increase its aggressiveness even more. Also the local oxidation of sulfides such as pyrite, often present in carbonate sequences, can generate sulfuric acid, boosting rock dissolution (Onac, 1991; Auler and Smart, 2003; Filipponi and Jeannin, 2006; Tisato et al., 2012, Audra et al., 2015). Sulfuric acid also reacts with other minerals such as clays and can cause the formation of a typical suite of

* Corresponding author.

E-mail addresses: jo.dewaele@unibo.it (J. De Waele), audra@unice.fr (P. Audra), giuliana.madonia@unipa.it (G. Madonia), marco.vattano@unipa.it (M. Vattano), lukas.plan@nhm-wien.ac.at (L. Plan), ilenia.dangeli@alice.it (I.M. D'Angeli), jcnobecourt@free.fr (J.-C. Nobécourt).

Table 1
Examples of the main sulfuric caves in the world.

| | | |
|---|----------------------------|--|
| Lower Kane Caves | USA (WY) | Egemeier (1981) and Engel et al. (2004) |
| Carlsbad Caverns, Lechuguilla Cave, etc. | USA (NM) Guadalupe Mts. | Hill (1987, 1990), Polyak et al. (1998), Palmer and Palmer (2000), Polyak and Provencio (2001), Engel et al. (2004), Calaforra and De Waele (2011), Palmer and Palmer (2012) and Kirkland (2014) |
| Glenwood Cave | USA (CO) | Barton and Luiszer (2005) and Polyak et al. (2013) |
| Cueva de Villa Luz | Mexico, Tabasco | Hose and Pissarowicz (1999) and Hose et al. (2000) |
| Movile Cave | Romania, Dobrogea | Sarbu et al. (1994, 1996) |
| Frasassi Cave | Italy, Umbria | Galdenzi and Menichetti (1995) and Galdenzi and Maruoka (2003) |
| Monte Cucco and Faggeto Tondo caves | Italy, Umbria | Galdenzi and Menichetti (1995) and Menichetti (2011) |
| Acquasanta Terme caves | Italy, Marche | Galdenzi et al. (2000) and Jones et al. (2014) |
| Montecchio Cave | Italy, Tuscany | Piccini et al. (2015) |
| Monte Soratte caves | Italy, Latium | Mecchia (2012) |
| Cala Fetente caves | Italy, Campania | Forti (1985) and Forti et al. (1989) |
| Santa Cesarea Terme caves | Italy, Apulia | De Waele et al. (2014) |
| Grotta di S. Angelo | Italy, Calabria | Galdenzi (1997) |
| Serra del Gufo-Balze di Cristo | Italy, Calabria | Galdenzi (1997) |
| Iglesiente mine caves | Italy, Sardinia | De Waele and Forti (2006) and De Waele et al. (2013) |
| Chevalley – Gr. des Serpents | France, Savoie | Audra et al. (2007) |
| Kraushöhle | Austria, Styria | Plan et al. (2012) |
| Bad Deutsch Altenburg caves | Lower Austria | Plan et al. (2009) |
| Diana Cave and Cerna caves | SW Romania | Onac et al. (2009, 2013), Wynn et al. (2010) and Puscas et al. (2013) |
| Provalata Cave | Rep. Macedonia | Temovski et al. (2013) |
| Aghia Paraskevi caves | N Greece, Kassandra | Lazaridis et al. (2011) |
| Rhar es Skhoun, Azrou massif | Algeria | Collignon (1983, 1990) |
| Nowi Afon Cave | Georgia, Abkhazia | Dublyansky (1980) |
| Cupp Coutunn Cave | Turkmenistan | Maltsev and Malishevsky (1990) |
| Tirshawaka Cave | N Iraq | Stevanović et al. (2009) |

minerals including the sulfates jarosite, alunite, and basaluminite, and the silicate halloysite. Some of these minerals, especially those containing potassium such as alunite and jarosite, can be dated with radiometric methods (Polyak et al., 1998). Also gypsum can be dated using the U/Th method (Sanna et al., 2010; Piccini et al., 2015). Timing of minerogenesis roughly corresponds to the age of cave formation, certainly when the SAS process was active. Thus, SAS by-products offer a unique opportunity to date speleogenetic phases, whereas other classical methods relying on dating of the cave filling, only post-date the cave itself.

Sulfuric acid caves are thus often intimately related to the contact zone between the water level, from which H₂S rises, and the air. Enlargement of the voids mainly happens due to condensation–corrosion processes in a highly acidic environment (Audra et al., 2007; Puscas et al., 2013). Condensation is greatly enhanced in the presence of thermal differences between the upwelling waters and the cave walls and atmosphere, even in low thermal environment where the thermal gradient reaches only a few degrees Celsius (Sarbu and Lascu, 1997; Gàzquez et al., 2015). Dissolution of carbonate rock in these conditions is extremely fast compared to normal epigenetic caves and can cause the formation of sizeable cavities in probably only a few thousands of years, about 1 or 2 orders of magnitude faster than the time needed to develop a normal meteoric cave. Most cave development occurs close to where sulfidic waters enter the carbonate rocks from below in areas where oxidation gives rise to sulfuric acid. Many SAS caves are water table caves, i.e. they formed along the more or less horizontal plane of the sulfidic

groundwater level (Audra et al., 2009a,b). Fluctuations of this level can cause these karst systems to exhibit stacked cave levels, indicating the rise or fall of the groundwater.

This paper deals with the detailed morphological and mineralogical description of four such SAS water table caves, one in France, one in Sicily, and two in Austria, and highlights their importance in the understanding of past hydrological and geomorphological conditions (Fig. 1).

2. Study areas

2.1. Grotte du Chat

The Grotte du Chat opens at 940 m a.s.l. in the southern French Alps at Daluis, Alpes-Maritimes. It is perched about 100 m above the Riou Gorge, a small tributary of the Var River. There are gentle slopes above the cave and the gorge below the cave, with its unstable slopes, probably corresponds to a Quaternary entrenchment.

The cave develops in an 80 to 100 m-thick Barremian (Lower Cretaceous) limestone sandwiched between thick marl layers belonging to the sedimentary cover of the Argentera–Mercantour basement. This unit is slightly folded but displays in detail complex structures. In the vicinity of the Grotte du Chat, a half-dome is cut by the Rouaine active sinistral fault (Fig. 2). To the east, the Barremian limestone crops out along the Var Valley slopes, representing the recharge area of the aquifer. To the west, the Barremian limestone strata are confined by the half dome plunge forming a discharge area where limestone is cut by the Riou Gorge and where water can rise from depth along the Rouaine Fault (Fig. 3). A Triassic gypsum diapir crops out less than 1 km to the south at Daluis village.

In the Riou Gorge at 840 m a.s.l., the thermal spring (18 °C) discharges 2–6 L/s. It is 7 °C above the local mean annual temperature that would correspond to a deep water circulation loop of at least 200 m. Water chemistry is of carbonated-chloride–sulfate type (Table 2). Significant hydrogen sulfide content gives a typical rotten-egg smell and sulfur bacterial mats are present.

The cave is well known and was first surveyed at the end of the 19th century. Ducluzaux (1994) observed upward developing morphologies



Fig. 1. Location of the studied SAS caves: 1. Grotte du Chat; 2. Kraushöhle; 3. Bad Deutsch Altenburg; and 4. Acqua Fitusa.

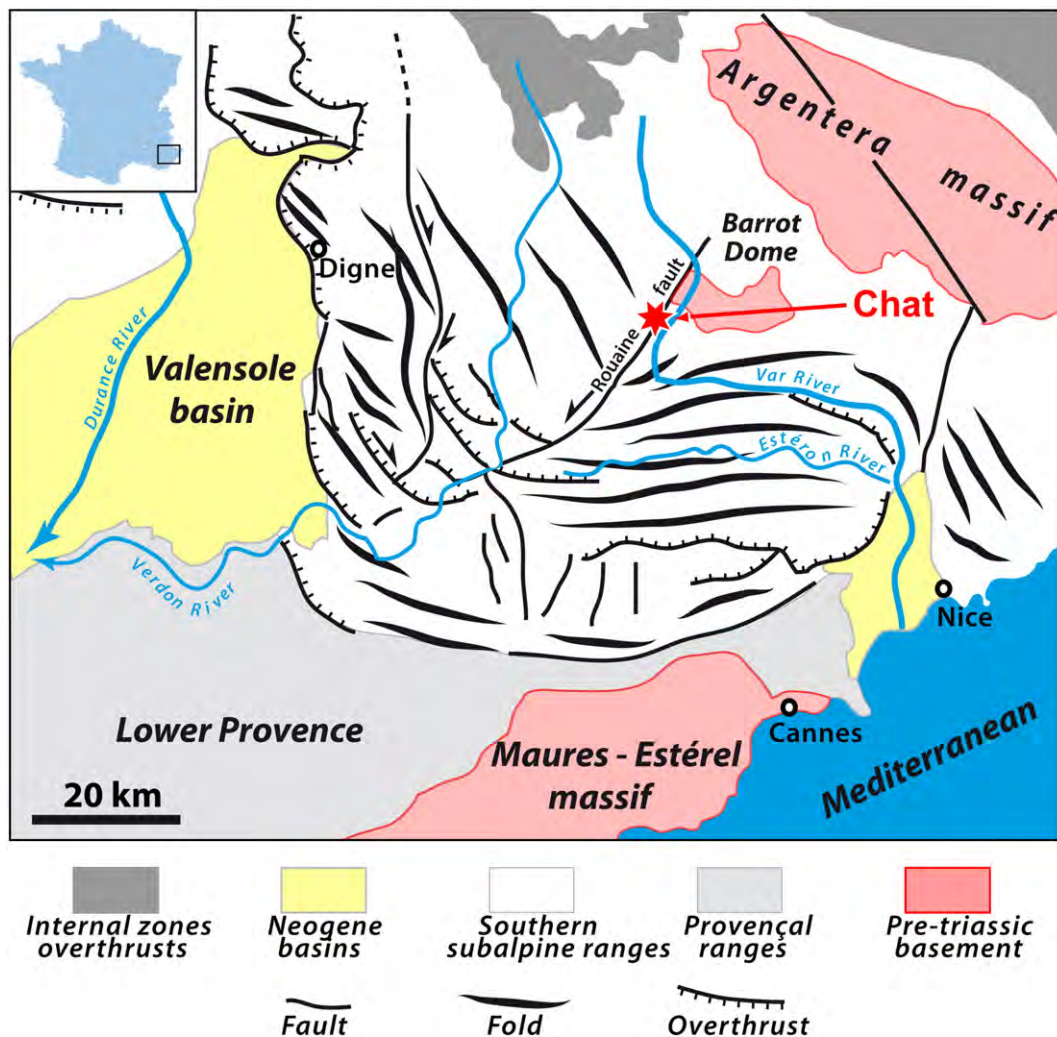


Fig. 2. Structural frame of the Castellane Arc in the Southern Alps (after Kerckhove and Roux, 1976). The Grotte du Chat locates along the active Rouaine Fault.

(i.e. cupola), the absence of connection to a surficial catchment, the presence of a thermal spring in the gorge and suggested a hydrothermal origin. Recent studies (Audra, 2007; D'Antoni-Nobécourt et al., 2008) confirm this origin, showing its SAS origin with a main development by condensation–corrosion producing specific features (i.e. cupola, replacement pockets, corrosion tables).

Grotte du Chat develops as a horizontal maze following the fracture network and extends to the west (Fig. 4). The Tables Chamber in the center is one of the main cave volumes. In detail, it is organized as tiers, the uppermost ones being upstream and to the west. The cave profile is horizontal with a tiny gradient (0.65%) toward the entrance.

2.2. Acqua Fitusa Cave

Acqua Fitusa Cave is located in the eastern sector of the Sicani Mountains, in the territory of San Giovanni Gemini (Agrigento province, central Sicily). The cave formed in the breccia member of the Upper Cretaceous Crisanti Formation (part of the basinal Mesozoic Imerese Domain), composed of conglomerates and reworked calcarenites with rudist fragments and benthic foraminifera (Catalano et al., 2013). The main entrance of the cave opens at 417 m a.s.l. on the eastern side of a fault line scarp that cuts a NNE–SSW oriented anticline that forms the La Montagnola Hill; this relief consists of rocks belonging to the Imerese Domain, overthrusting the succession of the Sicani Domain and the clastic Oligo–Miocene covers (Catalano et al., 2013) (Fig. 5). At the base of the Imerese and Sicani Domain Triassic interbedded

calclutites and marls with abundant pyrite and bitumen may occur. A luke-warm sulfuric spring opens at the base of the cliff at 380 m a.s.l., 300 m north of the cave entrance. The chlorine–sulfate–alkaline waters have a temperature of around 25 °C (Grassa et al., 2006). From spring to early autumn the entrance room of the cave hosts a large breeding colony of bats, including *Myotis myotis* and *Miniopterus schreibersii* (Mucedda pers. comm.), that produce significant amounts of guano. The cave contained numerous lithic fragments, remains of food and burials of Paleolithic and Chalcolithic periods (Bianchini and Gambassini, 1973). The first detailed exploration, description and cave survey was produced by the Gruppo Speleologico Agrigento (Lombardo et al., 2007). According to a more recent survey made in 2011 (Vattano et al., 2013), the cave consists of at least three stories of sub-horizontal conduits, displaying a total length of 700 m, and a vertical range of 25 m (Fig. 6). The main passages are generally low and narrow and follow sets of joints oriented in ENE–WSW, E–W and N–S directions, except when they merge producing large volumes such as at the entrance room. Very small passages develop from these galleries forming incipient mazes.

2.3. Kraushöhle

Kraushöhle opens east of the village Gams bei Hieflau in the north of the Austrian province of Styria (Fig. 7). It is the only known cave of SAS origin in the Northern Calcareous Alps, which is part of a more than 2 km-thick sequence of Permo–Mesozoic sediments. Middle and

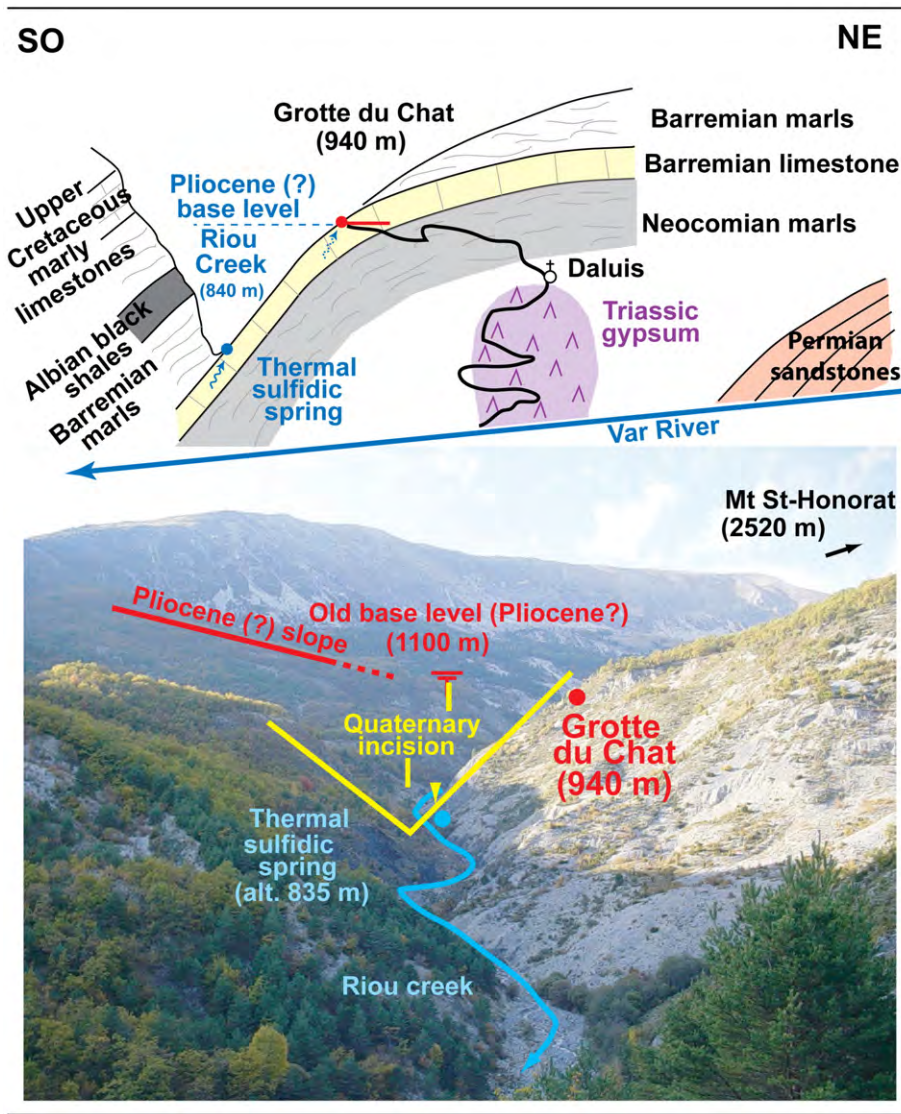


Fig. 3. Schematic structural frame of Grotte du Chat, view from Daluis village. The Barremian limestone, sandwiched in between thick marls is confined to the west where the thermal spring discharges along the Rouaine Fault (not visible, parallel to this view). Daluis village is located 1 km in the foreground on a Triassic gypsum diapir. The cave acted as a thermal outlet before the Quaternary entrenchment of the Riou Gorge.

Upper Triassic carbonates dominate this sequence, but Kraushöhle developed in a small tectonic wedge of the Lower Jurassic Hierlatz Formation, a limestone that is often developed as a reddish crinoid spar.

Table 2

Data of the thermal spring of Riou Gorge, Daluis [sampl. 3489, Laboratoire de l'Environnement, Ville de Nice, 20/03/06].

| | |
|---|------------|
| pH | 7.6 |
| Temperature (°C) | 17.5 |
| Conductivity (µS/cm) | 576–691 |
| Calcium (Ca ²⁺) | 40.3 mg/L |
| Magnesium (Mg ²⁺) | 8.7 mg/L |
| Sodium (Na ⁺) | 51.4 mg/L |
| Potassium (K ⁺) | 1 mg/L |
| Chloride (Cl ⁻) | 27 mg/L |
| Sulfates (SO ₄ ²⁻) | 36.4 mg/L |
| Nitrates (NO ₃ ⁻) | <1 mg/L |
| Sulfides (S ²⁻) ^a | 1.7 mg/L |
| Bicarbonates (HCO ₃ ⁻) | 234.2 mg/L |
| Fe total | 22 µg/L |
| Cu total | <10 µg/L |

^a Corresponding to 1.8 mg/L H₂S.

The cave opens at 616 m a.s.l. at the end of a narrow gorge of the Gams Brook. A H₂S-rich luke-warm spring emerges 93 m below the cave entrance and 1 m above the brook. A connection of the uprising hydrothermal water to the 400 km-long SEMP-fault system (Salzachtal–Ennstal–Mariazell–Puchberg) with its main strand 5 km to the south, can only be speculated.

Exploration of Kraushöhle started in 1881 and already Hauer (1885) and Kraus (1891) proposed a speleogenetic connection to the sulfur-bearing spring and set up a model for the replacement of limestone by gypsum as a cave forming process. One hundred years later this was confirmed by sulfur isotope studies by Puchelt and Blum (1989). Detailed studies of the cave morphology, mineralogy, cave wall alteration and age dating further confirmed the SAS origin (De Waele et al., 2009; Plan et al., 2012). They were accompanied by a resurvey of the cave that gave a length of 793 m and a vertical range of 53 m.

The cave consists of two central chambers – the larger one (Main Chamber) measures 50 × 15 m – from which several, partly interconnected, slightly inclined galleries branch off forming a 3D-maze (Fig. 8). The galleries and several chimneys terminate abruptly and the highest, the so-called Crystal Chimney, reaches 30 m above the Main Chamber (Fig. 8).

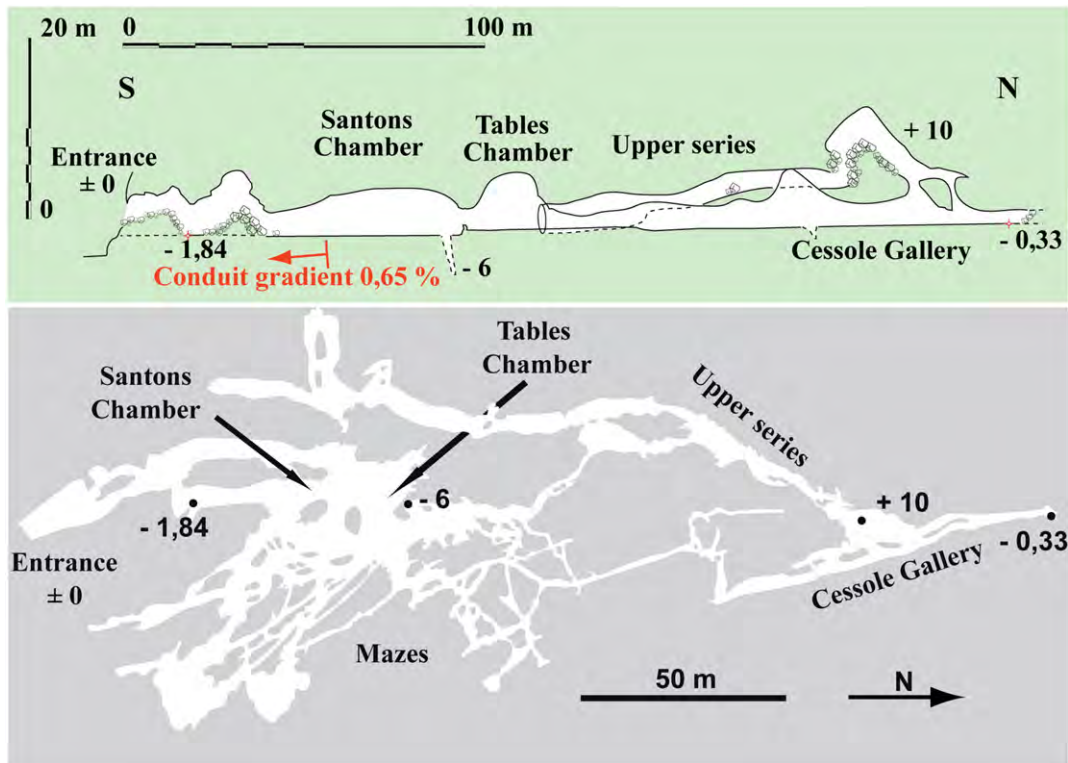


Fig. 4. Survey of Grotte du Chat: the typical low gradient profile is visible on the vertical profile (top), while the incipient maze is clear in plan view (below).

2.4. Bad Deutsch Altenburg caves

Bad Deutsch Altenburg is a village at the Danube River in the easternmost part of Austria only 15 km west of the Slovak capital Bratislava. It is located at the eastern margin of the Vienna Basin, which is a Miocene pull-apart structure. Along the margins of the southern part of this up to 6 km-deep sedimentary basin, several thermal springs emerge. Since Pre-Roman times the sulfur-bearing thermal water (up to 24.6 °C; 8 L/s) has been used for spas in Bad Deutsch Altenburg. The adjacent Hainburger Berge are part of the Tatricum (a Paleozoic–Lower Mesozoic crustal thrust sheet of the Central Western Carpathians) and at Bad Deutsch Altenburg weakly metamorphic Triassic dolomite crops out. The springs emerge at the border of the permeable carbonates and overlying Miocene clays and marls aquiclude. The mineralization and thermal heating of the water is explained by a circulation system within the carbonates that

are underlain by the crystalline basement of the Hainburger Berge (Fig. 9; Wessely, 1993).

Eight relatively small caves were opened during quarrying, the 121 m-long and 13 m-deep Stephanshöhle being the longest of them. The caves are restricted to a rather small area. Accessible caves are dry but are located only a few meters above the high water level of the (regulated) Danube. Unfortunately a 12 m-long cave (Tiefetagenhöhle) that reached into the present ground water of the Danube, was accessible in 1992 for a few months only and was removed by quarrying works before further investigations were possible.

A systematic survey of most caves in this area was conducted in the late 80s (Mayer and Wirth, 1989) and they were attributed to SAS by Plan et al. (2009).

The caves are rather narrow and cross-sections are in the order of 1 m². They developed along sets of W(NW)–E(SE) and NNE–SSW

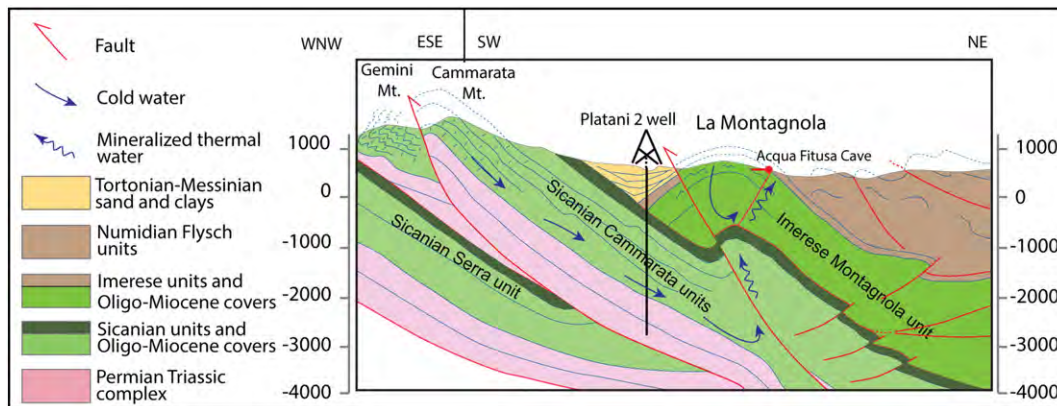


Fig. 5. Geological section of the La Montagnola area and location of Acqua Fitusa Cave. Modified from Catalano et al. (2013).

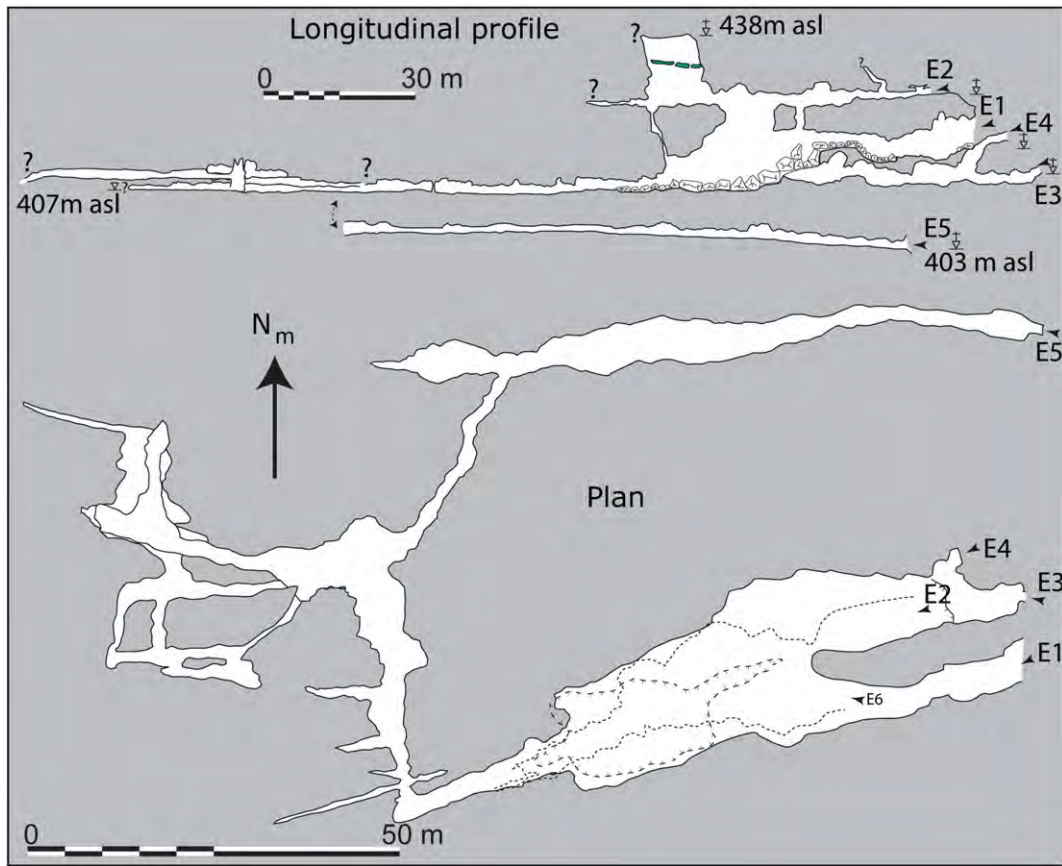


Fig. 6. Survey of Acqua Fitusa Cave.

trending faults and joints at several sub-horizontal stories between 142 and 162 m a.s.l. with distinct water table notches (Fig. 10).

3. Methods

All caves were mapped using traditional caving techniques (compass, clinometer and laser range finder for distances). This delivers cave maps with an accuracy of about 1%. Detailed mapping with a water tube level and laser range finder allowing centimeter accuracy were used for vertical referencing of corrosion notches. Typical meter- to centimeter-sized cave morphologies were mapped and measured, and photographic documentation completed the observations.

Cave minerals and weathering products on the walls were sampled for mineralogical analysis. Samples were analyzed using a Philips PW 1050/25 X-ray diffractometer (XRD, 40 kV and 20 mA, CuK α radiation, Ni filter) at the University of Modena and Reggio Emilia, Italy, and on a Philips diffractometer (XRD, 40 kV and 20 mA, CoK α radiation, Graphite filter) at the CEREGE-CNRS, Aix-en-Marseille, France.

Samples of gypsum were analyzed for sulfur stable isotopes at the ETH Zurich with a Thermo Fisher Flash-EA 1112 coupled with a ConFlo IV, interfaced to a Thermo Fisher Delta V Isotope Ratio Mass Spectrometer (IRMS). Isotope ratios were calibrated with the reference materials NBS 127 ($\delta^{34}\text{S} = +21.1\text{‰}$), SO_5 ($\delta^{34}\text{S} = +0.49\text{‰}$) and SO_6 ($\delta^{34}\text{S} = -34.05\text{‰}$) and are reported in the conventional δ -notation with respect to V-CDT (Vienna Cañon Diablo Troilite) (measurement reproducibility was better than 0.3‰).

Alunite of Kraushöhle was dated using the $^{40}\text{Ar}/^{39}\text{Ar}$ method similar to that from Polyak et al. (1998) and was previously reported in De Waele et al. (2009).

4. Results and discussion

4.1. Cave pattern

The four described caves are characterized by an anastomotic or maze pattern following a network of fractures (Figs. 4, 6, 8 and 10). The caves developed along the fractures through which acidic fluids were discharged, resulting in more or less elongated anastomotic cave passages with the discharging feeders along their path. In Kraushöhle these feeding fissures are no longer clearly visible, as they are mainly covered by sediments. If the rising fluids were delivered through more fractures a maze cave developed, such as is the case in all caves but Kraushöhle. The larger rooms are located along the major feeding fractures and often at their intersection.

Grotte du Chat, Acqua Fitusa, and the Bad Deutsch Altenburg caves represent typical examples of inactive SAS water table caves (Audra et al., 2009a,b). Kraushöhle, although showing some minimal epigenic overprinting, also has many of the typical characteristics of a SAS water table cave. Despite their relatively small size, all these caves are very interesting for the abundance and variety of morphologies and deposits formed at and above the water table where H_2S degassing and thermal convection produced strong condensation–corrosion processes (Table 3).

4.2. Feeders and corrosion along standing pools

Where visible, thermo-sulfuric discharge points breach the flat floor of the cave passages and are normally not large enough to allow a person to pass (Fig. 11A). These feeders tend to pinch out at shallow depth, since most of the corrosion occurs where H_2S can convert into sulfuric acid in an oxidizing environment. Only in Acqua Fitusa Cave some of these feeders, located at different levels of the cave, are large

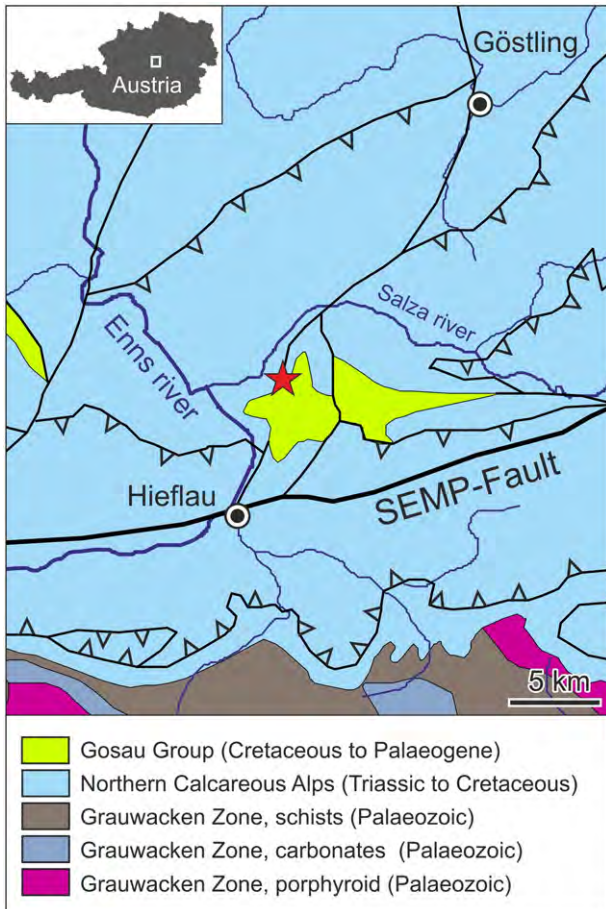


Fig. 7. Geological sketch map and location of Kraushöhle (star). Modified after Schuster et al. (2013).

enough to be explored to a depth of over 10 m. The walls of one of these feeding fissures are covered with a network of calcite “roots” (Fig. 11B). Upstream of the last discharging fissures, the passage normally comes soon to a dead end since aggressive power of the fluids diminishes with the distance from their injection point into the subaerial part of the cave (Fig. 12). The largest cave volumes are located above and downstream of the feeders, similar to existing active SAS caves such as Cueva de Villa Luz (Hose and Pisarowicz, 1999) and Lower Kane caves (Egemeier, 1981).

When the water level drops these feeding fissures can still act as thermal vents, if warm water is below the passage. Rising vapors will cause condensation–corrosion processes on the cooler overlying walls and roof, whereas evaporation processes occur only at the edges of the feeders by subsident cooler and drier air leading to the deposition of calcite as popcorn rims (Fig. 16).

When the water level rises to the surface in the enlarged cave, and when the amount of H_2S is significant, the uppermost part of the water column will always be much more aggressive than the deeper one. Also condensation runoff from the walls can continuously feed acidic fluids to the pools. If the water level is stable enough, these pool surface waters will cause lateral corrosion of the limestone bedrock creating notches with a flat roof (Fig. 11C).

4.3. Main cave volume developed by condensation–corrosion

While cave enlargement is relatively subdued in phreatic conditions, oxidation of H_2S and formation of sulfuric acid is particularly efficient in the aerated environment, causing extensive corrosion of the cave walls and roof.

The volume of dissolved limestone due to corrosive flowing water in the feeders and the pools is limited compared to that produced by the condensation–corrosion processes that appear to be responsible of most of the volume. Several micro- and macromorphologies generated by condensation–corrosion processes above the water table, can be observed in all SAS caves (Galdenzi, 2001; Audra, 2008). They are particularly well developed above the feeders, but also in Kraushöhle, where these are no longer visible.

Ceiling cupolas and large wall convection niches occur in the biggest rooms of both Kraushöhle and Grotte du Chat (Fig. 13A). This expansion driven by condensation–corrosion may also cause the formation of pendants at junctions of several cupolas or between braided channels. The ascending air flow is responsible for the formation of megascallops, a wave-like corrosional pattern along the roof and the walls, similar to scallops of phreatic flow origin but at least ten fold larger (Fig. 13B). Above the main feeding points, especially when rising fluids are warm and rich in H_2S and the thermal gradient is high, condensation–corrosion at the ceiling can be very strong leading to the development of rounded dome-like chambers. This is clearly visible in Grotte du Chat (Fig. 13C). Ceiling cupolas and spheres represent convection cells in which condensation is more abundant at the cooler ceiling, heavily increasing their upward development. These ceiling spheres are typical of thermal caves such as those described in Chevalley and Serpents caves in France (Audra et al., 2007) but initially mentioned in Hungary (Szunyogh, 1990) where they have been interpreted as a result of phreatic convections.

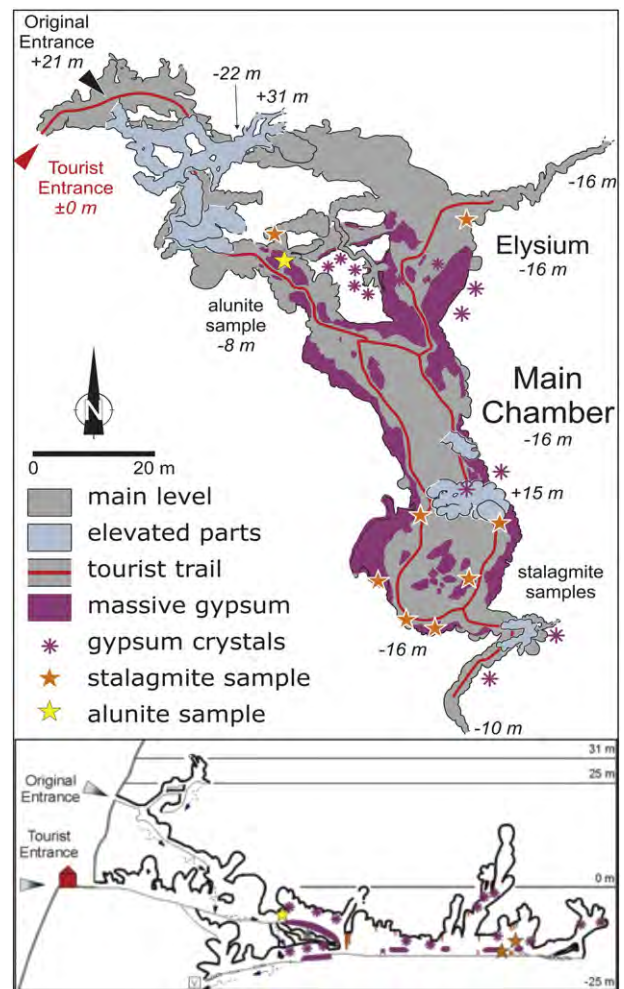


Fig. 8. Plan and longitudinal profile of Kraushöhle.

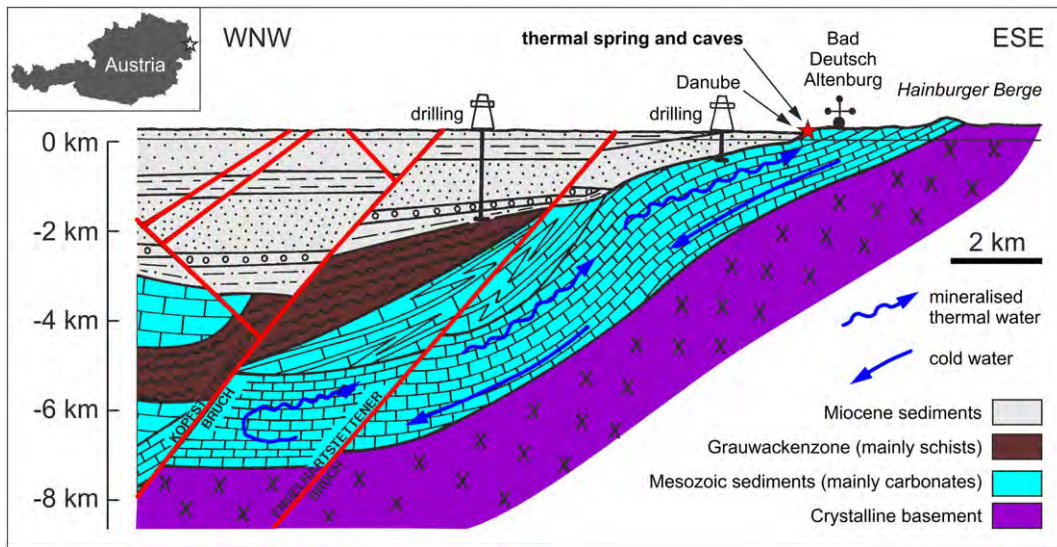


Fig. 9. Geological section showing the proposed circulation system of the thermal water of Bad Deutsch Altenburg. Modified after Wessely (1993).

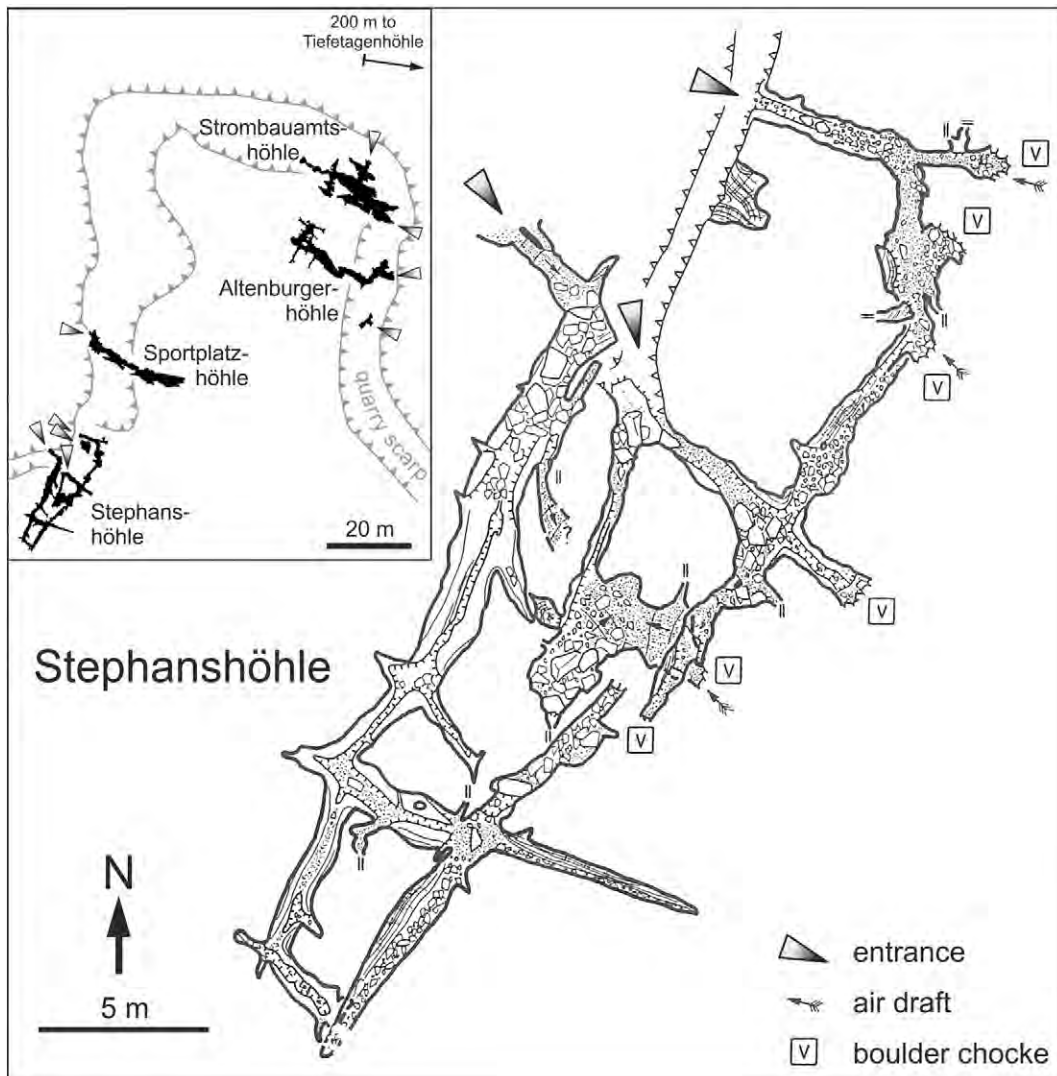


Fig. 10. Survey of Stephanshöhle, the main cave at Bad Deutsch Altenburg.

Table 3
Typical sulfuric acid cave morphologies in the four described caves. Note not all forms are exclusive to SAS caves.

| Cave morphology | Grotte du Chat | Acqua Fitusa Cave | Bad Deutsch Altenburg caves | Kraushöhle |
|---------------------------------|----------------|-------------------|-----------------------------|------------|
| Maze cave | x | x | x | x |
| Elongated anastomotic passage | | | | x |
| Feeders | x | x | x | |
| Sulfuric acid chimney | | | | x |
| Sulfuric notches with flat roof | | x | | x |
| Wall convection niches | x | x | x | x |
| Ceiling cupolas | x | x | | x |
| Condensation–corrosion channels | x | x | | x |
| Megascallops | x | x | | x |
| Condensation domes | x | x | | x |
| Boxwork | x | x | x | x |
| Weathered walls | x | x | x | x |
| Replacement pockets | x | x | x | x |
| Sulfuric karren | x | x | | x |
| Ceiling pendant drip holes | | | | x |
| Sulfuric cups | | x | | x |
| Corrosion tables | x | x | x | x |
| Replacement gypsum crusts | x | x | | x |
| Calcite popcorn | x | x | | |

When the ceiling of the developing rooms becomes higher, warm air flow will follow the overhanging walls to reach the highest parts. Condensation on the walls will be higher in these places gradually carving a condensation–corrosion channel. These ceiling channels resemble paragenetic ceiling half-tubes (Renault, 1968; Pasini, 2009) or some shallow bubble trails (Chiesi and Forti, 1987; De Waele and Forti, 2006; Audra et al., 2009c; Ginés et al., 2014) but have a different origin. Condensation–corrosion channels are often sculpted with a set of megascallops that are absent in the last two types of channels. They are also common

in thermal caves, and have also been reported in a Mexican cave above guano deposits, where exothermic reactions produce the rising of warm air rich in carbon dioxide (Forti et al., 2006). These convective air flows and related condensation processes can explain the rounded shapes of cross-sections that are easily confused with passages due to phreatic water flow.

4.4. Cupolas, domes and chimneys, the upward feedback

Ceilings are the coolest places, being more distant to the thermal source. Consequently, the largest amount of condensation, and thus corrosion, occurs on the ceilings above the feeders, causing a positive feedback in favor of upward expansion of cupolas that evolve in domes or chimneys (Fig. 14). Condensation waters then flow along walls and concentrates as dripping from pendants that feed a water film smoothing the corrosion table. On the contrary the lowest roofs remain warm, causing less condensation, thus remaining dryer. Their corresponding floors, also dry, may retain gypsum deposits, as replacement pockets or thick crusts (Fig. 15A).

4.5. Medium-scale condensation–corrosion morphologies

Deep and more or less horizontal wall convection niches are present at different heights on the cave walls of many passages. In some places these niches coalesce and align forming notches (Fig. 15A). These are formed by rising air above a thermal pool, creating convection cells that focus condensation–corrosion processes. Dimensions of these sub-hemispheroidal niches are homogeneous, and they are roughly aligned at the same level.

In general, condensation–corrosion attacks the massive limestone uniformly, slowly weathering (by dissolution) the rock and leaving a powdery residue. In some cases it is possible to scratch the walls because the limestone has become soft. When mineral veins or fossils

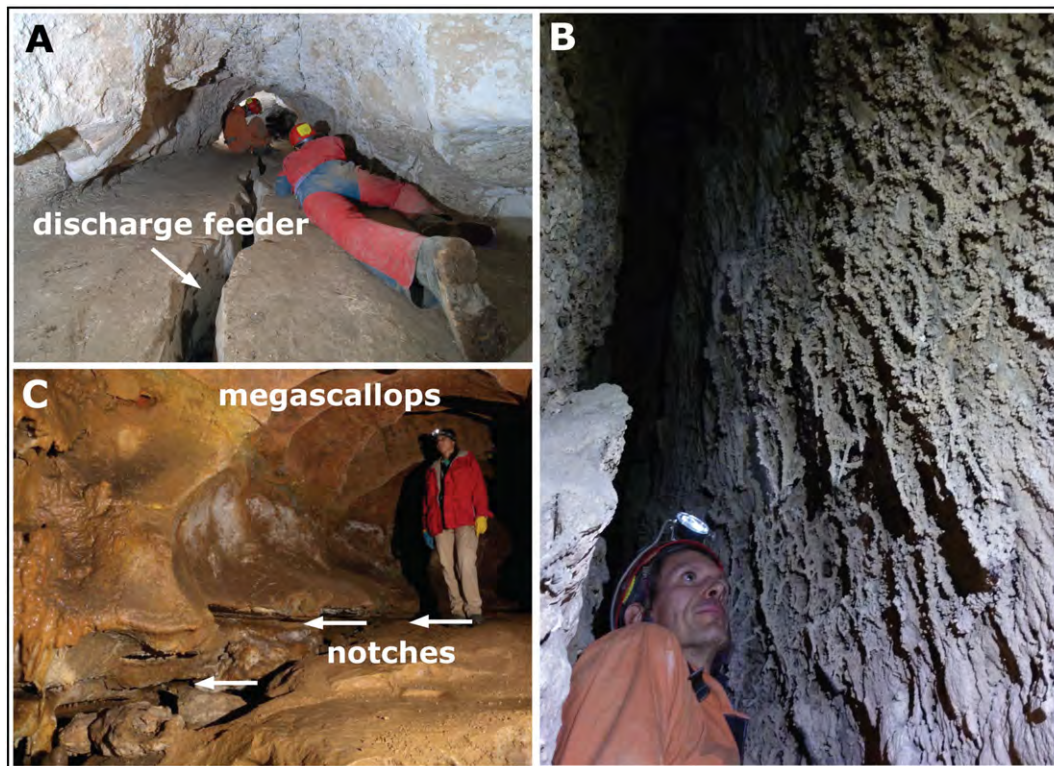


Fig. 11. Morphologies in typical SAS water table caves: A. Thermo-sulfuric feeding fissure cutting planar ground in Acqua Fitusa Cave; B. the curious subaqueous root-like calcite speleothems in Acqua Fitusa Cave; and C. passage sculpted with megascallops: note the notches with flat roof at the bottom of the passage, Kraushöhle.

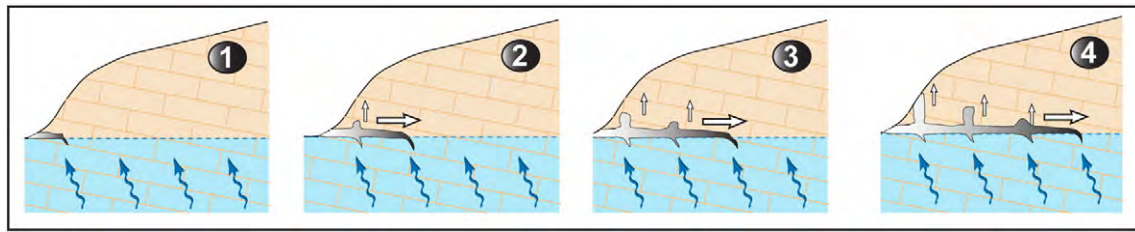


Fig. 12. Longitudinal development of a SAS water table cave: regression of the discharge point causes the conduit to retreat ending blindly upstream of the last sulfidic feeder.

are present, condensation–corrosion will attack the rock in a differential way, creating boxworks and exposing fossils in relief (Fig. 15B).

Because condensation is often more abundant in the highest and cooler part of conduits, the differential corrosion is more pronounced on high walls and roofs. If condensation is strong, the water film will descend by gravity along the walls and increase its flow downward. This allows the sheet of water to wash the median parts of the walls, making them smoother and harder.

Replacement pockets due to corrosion–substitution processes are widespread in all caves (Fig. 15C). These are hemispherical corrosion features (Fig. 15E) with diameters of some centimeters to more than 1 dm embedded into the wall. They are formed by concentrated sulfuric

acid corrosion, with simultaneous replacement of calcite by microcrystalline gypsum (Galdenzi and Maruoka, 2003). These replacement pockets often still contain the original gypsum, except in the Bad Deutsch Altenburg caves. The fact that gypsum is absent in these caves is due to the subsequent flooding of the passages by the nearby Danube River.

This hygroscopic gypsum retains the sulfuric acid-rich fluids and allows corrosion to proceed, causing the progressive deepening of the pockets. When the gypsum falls off, the pockets become empty, and condensation–corrosion proceeds more slowly. The inner rock surface of the pockets is often very smooth and regular (Fig. 15D). These pockets are often distributed along a vertical range, becoming smaller

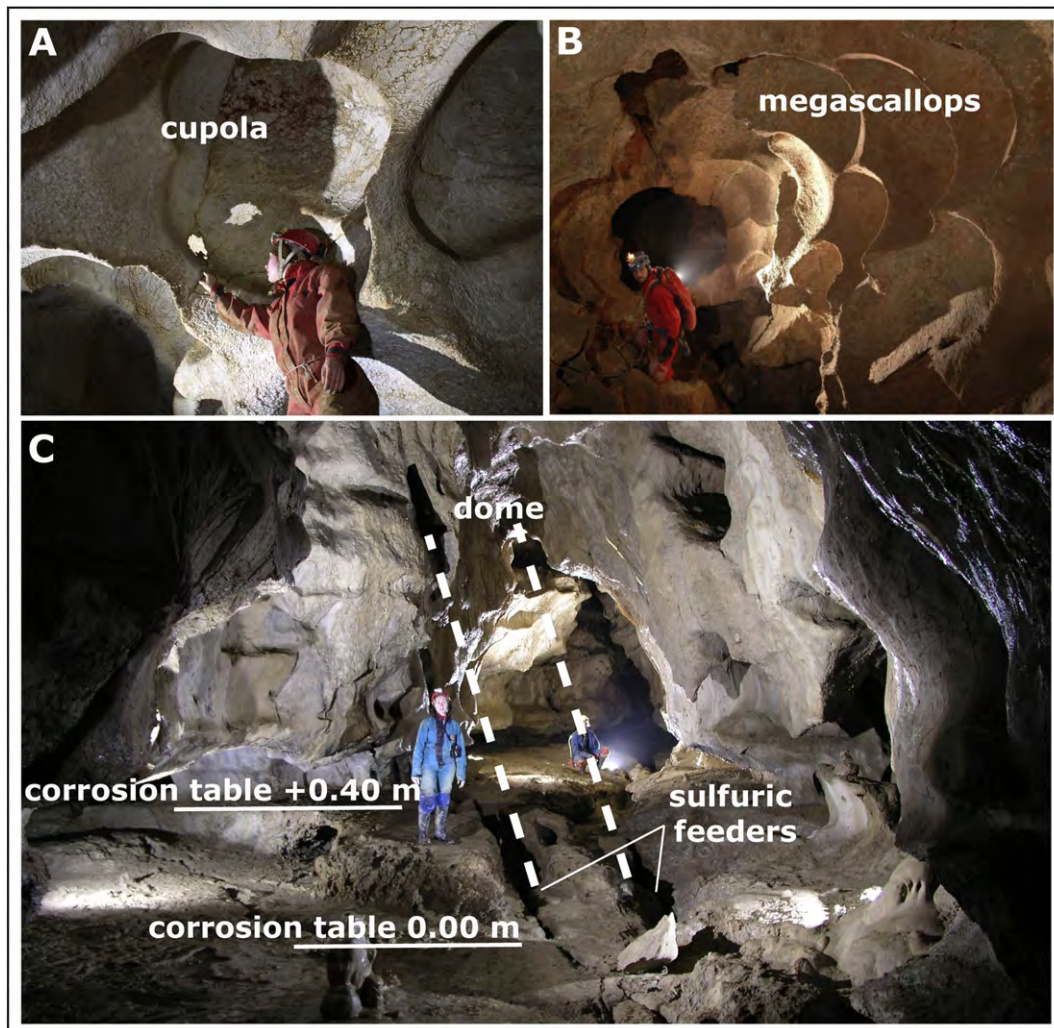


Fig. 13. Condensation–corrosion morphologies in SAS water table caves: A. Coalescing ceiling cupola in Kraushöhle; B. megascallops on the roof of a passage in Kraushöhle; and C. dome-like chamber and corrosion tables in Grotte du Chat.

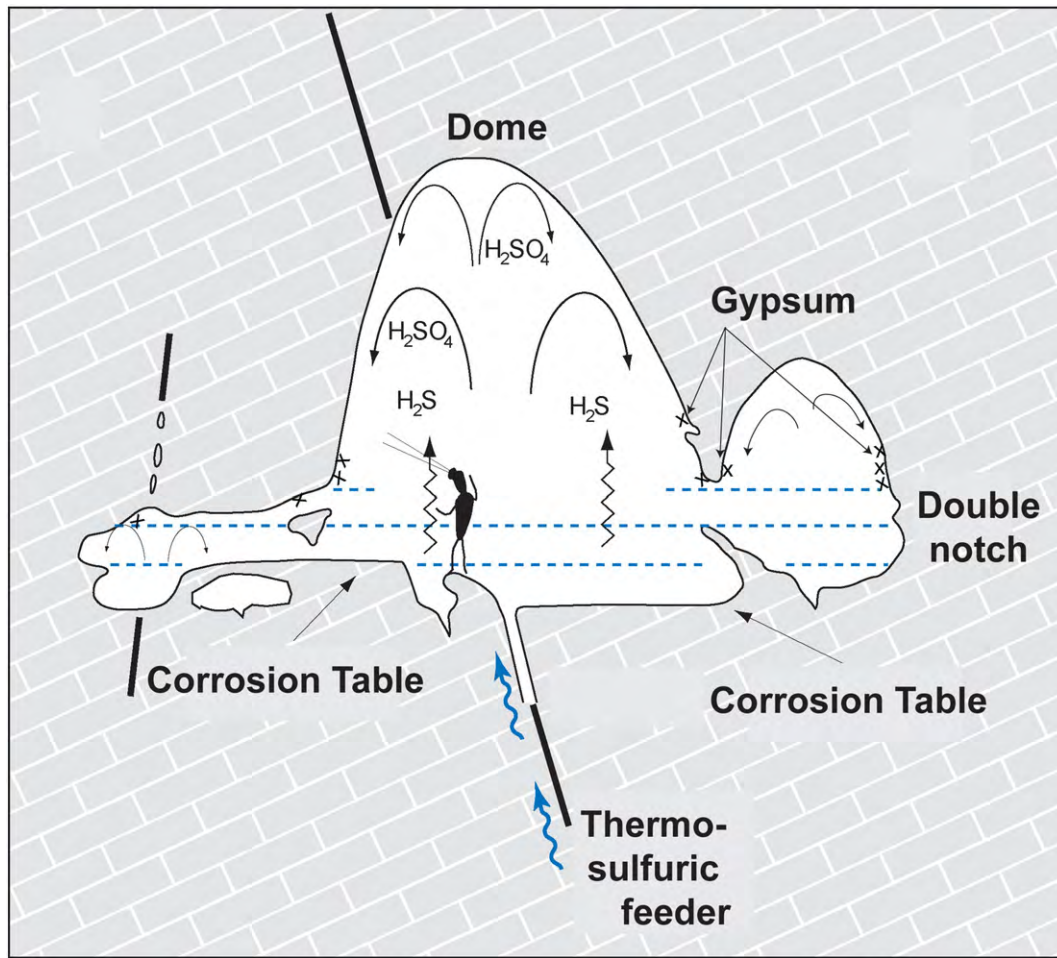


Fig. 14. The positive feedback of upward development of the highest ceilings. Dashed lines show variations in the water level. See text for explanation.

and ultimately disappearing in the lower and higher parts of the cave passage. This vertical distribution is related to the geometry of the walls and the possibility of gypsum to remain attached to the carbonate rock without being washed away or fall off. Their density is also higher around the feeders where H_2S degassing occurs.

Replacement pockets are diagnostic features of SAS, since they clearly differ from any other pockets or scallops made by diffuse corrosion of flowing water in epigenic or other hypogenic caves. Replacement pockets have a perfect hemispherical shape, and normally have a smooth inner surface. Only the ones in Bad Deutsch Altenburg caves show a pattern of mm-sized channels or ridges. In general they are distributed at middle height of the passage, and the walls in between the pockets are rather smooth.

4.6. Vertical distribution of features and deposits

The process of H_2S degassing and oxidation into sulfuric acid above the feeding point is driven by thermal convection cells. Rising warm air cools on the colder ceiling producing condensation, whereas the corresponding sinking air warms up and produces evaporation, similar to what happens in thermal caves (Sarbu and Lascu, 1997). On the ceiling, condensation moisture strongly corrodes the rock forming boxwork and causing the upward and lateral development of the passage. Condensation concentrates as downward runoff along walls transporting solutes, both carbonates from limestone wall dissolution and sulfates from replacement. This diffuse runoff along walls gradually increases downward. At middle-height of the passage, discrete areas protected from runoff allow local accumulation of sulfates and the development of replacement pockets. The pocket's density increases

downward following increasing evaporation. In the lower part of the passage, evaporation and high solute concentration allows continuous deposition of gypsum as thick crusts. In a similar way, in areas where evaporation dominates, calcite precipitates as cave popcorn (Caddeo et al., 2015). Finally, the floor displays a perfectly smoothed surface (glacis) resulting from highly corrosive sub-horizontal flow combining the aggressiveness from both the feeder and the dripping condensation. Such convective processes are responsible for the vertical distribution of features and deposits, which is also diagnostic for SAS (Fig. 16).

4.7. Concentrated sulfuric acid related features

In Grotte du Chat and in Kraushöhle the concentration of sulfuric acid in condensation waters and drip-rate were such to allow acid dripping from the roof, similar to what occurs in active SAS caves such as Cueva de Villa Luz (Hose et al., 2000). In this last cave droplets are produced at the end of mucolites and in biofilms, or seep through replacement gypsum crusts which prevent, at least to a certain extent, the acid attacking the ceiling carbonate rocks (Hose and Pizarowicz, 1999; Hose et al., 2000). In Grotte du Chat and Acqua Fitusa Cave these extremely acid drops have created a series of morphologies such as sulfuric karren and cups (Fig. 17D); similar features have also been found at the base of the Crystal Chimney in Kraushöhle (Plan et al., 2012) (Fig. 17A). On the floor of the "Wilczekgang" in this cave, unique 10 to 35 cm-wide bowl-shaped depressions surrounded by walls up to 15 cm high have been found (Plan et al., 2012). Since they are always located between 0.8 to 1.7 m below triple junctions of cupolas, forming pendants or lowest points along the ceiling, these have been called "ceiling pendant drip holes", probably also due to acid corrosion (Fig. 17C).

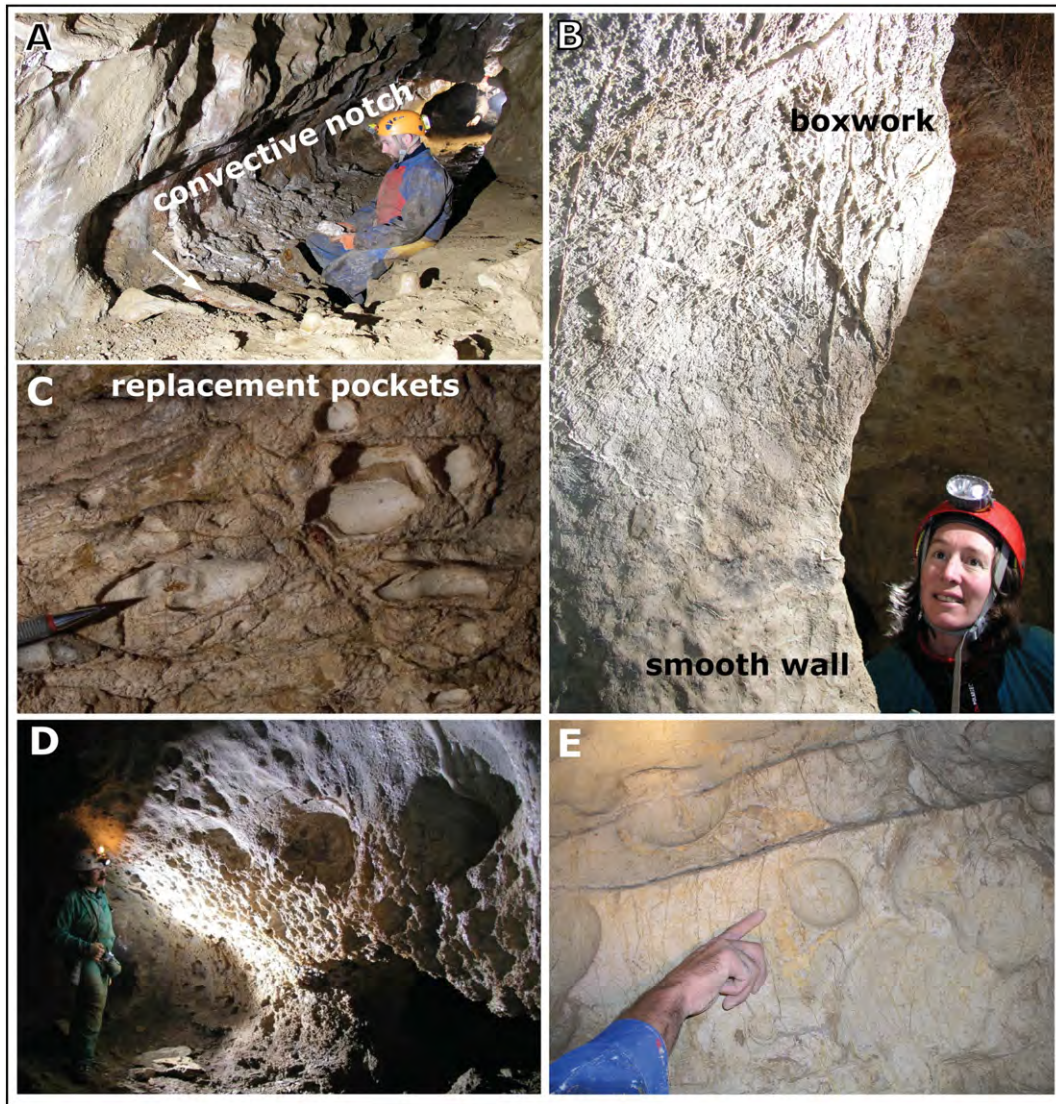


Fig. 15. Medium-scale condensation–corrosion morphologies in SAS water table caves: A. convection–corrosion notches in Grotte du Chat; note the white gypsum piled up at the bottom of the notch; B. boxwork in Grotte du Chat; C. typical replacement pockets on the roof above a corrosion table, Stephanshöhle, Bad Deutsch Altenburg; and D–E. replacement pockets located at half-height on the walls, Grotte du Chat.

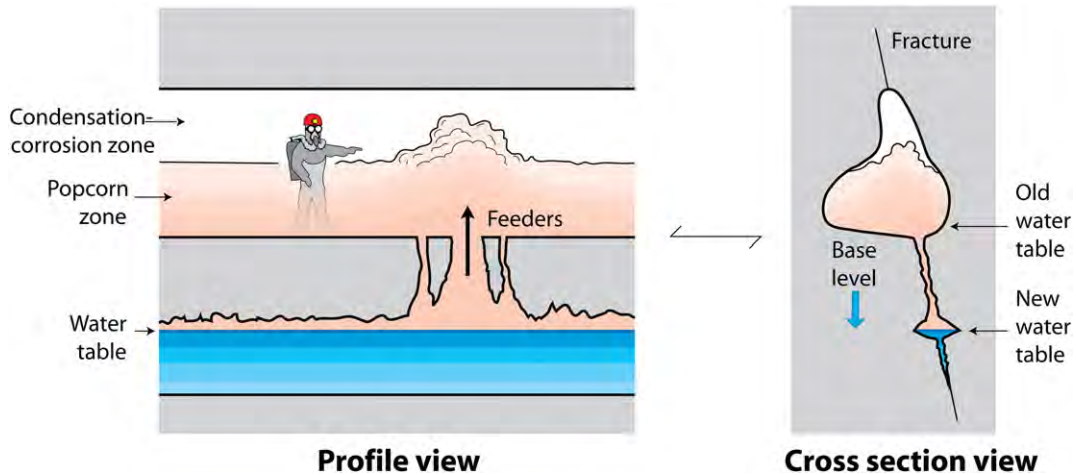


Fig. 16. Vertical distribution of wall features and popcorn according to aerial thermal convection loops that produce condensation–corrosion at the top of the passage and evaporation–precipitation in the lower parts. The cross-section (right) is typical of a SAS water table cave.



Fig. 17. Morphologies related to dripping or flowing acid water A. Sulfuric karren, Kraushöhle; B. corrosion table in Grotte du Chat cutting the dip of the limestones; C. ceiling pendant drip holes in Kraushöhle; and D. sulfuric karren and solution pans in Acqua Fitusa Cave (5 cm-long knife for scale).

Acid dripping water can also form drip tubes, half-cylinders carved along walls which originally projected into the rock mass as a full tube with a round bottom. These forms are very rare and have been seen in Kraushöhle.

A very special type of morphology related to the acid condensation waters flowing back to the feeding fissure (or pool) are the corrosion tables (Fig. 17B). These are almost perfectly horizontal surfaces of rock that have been flattened down by corrosion. This planation by sulfuric acid-rich waters creates smooth glacis, in which rocks of different hardness are worn down equally. Corrosion tables can be seen in all investigated caves, but are best developed and preserved in Grotte du Chat. The very small gradient of the corrosion tables both transversely (1.6%) and longitudinally (0.1 to 1.3%) results from a balance between turbulence and oxygenation. Steeper slopes allow water to flow with more turbulence enhancing oxygenation and thus formation of sulfuric acid by oxidation of dissolved H_2S . This will eventually lead to higher downwearing rates than in flatter surfaces, leading ultimately to the formation of an equilibrium slope (Egemeier, 1981). The altitude of these corrosion tables adjusts to a position slightly above that of the water level. If the sulfuric water level drops, the corrosion table will be entrenched, starting from the water level. Subsequent drops in water level can leave a set of distinct perched corrosion tables. In Grotte du Chat twelve levels are recorded within only 6 m of elevation (Audra, 2007).

4.8. Evolution of maze pattern by passage expansion and integration

The widespread and homogeneous dissolution by condensation–corrosion processes leads first to a widening of all open fractures and

joints close to or immediately above the discharging H_2S -rich fluids. This creates mazes, similar to the ones formed under epigenic phreatic conditions, but without signs of flowing water like scallops or coarse-grained allochthonous sediments. The evolution proceeds by expansion of volumes around sulfidic feeders while distant passages in the maze are less enlarged. The progressive expansion of neighboring passages leaves remnants of partings, with typical concave pillars, pendants, blades, projecting corners, arches, and half-tubes originating from integration of lateral tubes that resemble notches (Osborne, 2007). Depending on the distance from the discharging points, the passage sizes are irregular and the entrance into the largest chambers often occurs through narrow or seemingly incidental passages (Fig. 18).

4.9. Sulfate mineral by-products of SAS

The most abundant SAS mineral is gypsum which displays different shapes and colors. Saccharoid replacement gypsum crusts are common in many passages; the gypsum is located in large vertical fissures along the walls, it can partially cover wall convection notches, or replacement pockets. Large gypsum bodies are found on the floors of the biggest rooms in correspondence of which small ceiling cupolas and pendants are associated on the roof. In Acqua Fitusa Cave centimetric euhedral gypsum crystals have grown inside mud sediments, while in Kraushöhle a chimney rising above the central chamber hosts decimetric yellowish secondary gypsum crystals made by the washing of sulfates by condensation in higher parts followed by crystallization through evaporation in lower parts. Kraushöhle also hosts other sulfates such as alunite, jarosite and meta-alunogen, the hydroxide gibbsite, the silicate halloysite, and opal. Grotte du Chat hosts, besides gypsum, jarosite. All these minerals

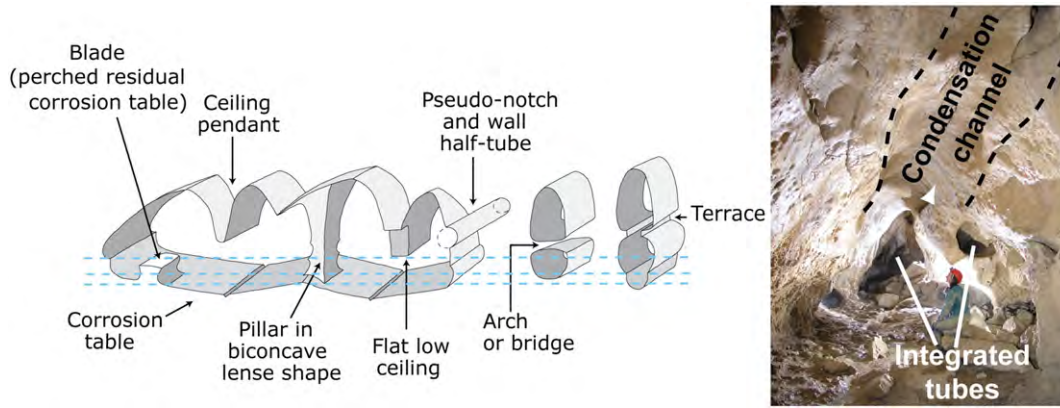


Fig. 18. Typical passage configuration of a SAS water table cave with narrows, partings and pillars. The dashed line shows variation in the water level.

are typical of low-pH conditions characteristic of SAS caves (Polyak and Provencio, 2001; Plan et al., 2012).

4.10. Sulfur stable isotopes

Stable sulfur isotopes of all caves (except Bad Deutsch Altenburg) are reported in Table 4, with values also for some other well-known SAS caves. Most of these data are consistent with bacterial sulfate reduction or thermochemical sulfate reduction of evaporitic rocks with hydrocarbons (i.e. methane) providing the source of electron donors producing H₂S. Two of the Acqua Fitusa Cave sulfates (both correspond to gypsum sampled in the upper level, while the ones with more negative values come from the lower level) show positive values, and testify the complexity of sulfur isotopic evolution similar to what has been documented in Cerna Valley (Wynn et al., 2010; Onac et al., 2011). These less negative values can derive from the hostrock or from the less fractionation during the transformation from sulfate to sulfide. Further stable isotope analyses would be required to better understand the behavior of the geochemical system.

4.11. Age of caves, cave levels and landscape evolution

SAS water table caves are exceptional recorders of the past position of the water table level. Several meso-morphologies, such as the notches with flat roof and the corrosion tables, are precise indicators of the exact position of the water table at the moment of their formation. Also the overall long-profile development of SAS water table caves, with a very low gradient from the upstream discharging points to the spring, allow to precisely locate the position of the ancient water tables. Horizontal cave passages can be dated in a direct way by constraining chronologically the secondary by-products of the SAS process, which were formed exactly at the time when acid-solutional processes were

active. Gypsum, the ubiquitous by-product of SAS, can be dated by U/Th methods (Sanna et al., 2010; Piccini et al., 2015) but the relatively low U content often does not allow precise ages to be determined. Alunite and jarosite, instead, often produced by the reaction of sulfuric acid with clay minerals hosted in the original carbonate sequence, can give useful results with the K/Ar and Ar/Ar methods (Polyak et al., 1998). Alunite has been dated at Kraushöhle and showed this cave, located around 80 m above the present thalweg and active sulfuric spring, to be less than 160 kyr old (Plan et al., 2012). Stalagmites that grew after the SAS processes stopped in the cave were dated by U/Th method and are at least 86 kyr old (Spötl et al., 2014). This testifies to a very rapid (0.5 to 1 m/kyr) entrenchment of the Gams Brook.

The age of the caves in Bad Deutsch Altenburg can only be speculated as they lack speleothems but they must be rather young, since the lowest accessible parts are only a few meters above the level of the Danube River.

5. Conclusions

Sulfuric acid water table caves are among the most interesting hypogenic caves in limestone and dolostone, from a biological and geological point of view. They have been reported from many regions of the world and typically display a suite of easily recognizable morphological and mineralogical characteristics (Table 5). Sulfuric acid produced both by abiotic and biotic oxidation of H₂S is rapidly neutralized by the carbonate host-rock, with the typical replacement of calcite by gypsum. These processes occur mainly in the aerated environment, close to and above the water level, where oxygen levels are high enough to oxidize the degassing H₂S rapidly. Rising waters are often slightly warm, boosting the condensation of water vapor above the feeding fissures. Some geomorphological features, such as blind-ending passages upstream of the discharge points, corrosion tables, replacement pockets, sulfuric cups and karren are unique to these caves. Also the presence of sulfates, mainly gypsum but also jarosite, alunite and others, are diagnostic features of SAS caves. Their speleogenetic evolution is closely related to the water table position and, because of their rapid evolution, they often are very precise records of base level changes. Some of the minerals typically present in these caves are formed during SAS speleogenesis and their dating precisely marks the age of cave formation, and thus of the base level position.

Acknowledgements

The exploration, survey and documentation in the caves have involved many cavers and cave photographers: Chris Berghold, Giuseppe Ceresia, Yuri Dublyansky, Simone Inzerillo, Iris Lenauer, Silvia Katzinger, Steffi Koppensteiner, Riccardo Presti, Angelo Provenzano,

Table 4
Stable sulfur isotopes of gypsum in the studied SAS caves and comparison with some other cave studies.

| Cave | δ ³⁴ S (‰) | Reference |
|--------------------|-------------------------------|-----------------------------|
| Kraushöhle | −23.12 to −15.83 | Puchelt and Blum (1989) |
| Acqua Fitusa Cave | −1.0 to +4.4 and 10.2 to 10.6 | This study |
| Grotte du Chat | −9.4 | Audra (2007) |
| Montecchio Cave | −28.3 to −24.2 | Piccini et al. (2015) |
| Lechuguilla Cave | −25 to +5 | Hill (1987) |
| Frasassi Cave | −20 to −8 | Galdenzi and Maruoka (2003) |
| Cueva de Villa Luz | −24.87 to −22.12 | Hose et al. (2000) |
| Provalata Cave | −2.3 to −1.9 | Temovski et al. (2013) |
| Cerna Valley Caves | −27.9 to +19.5 | Onac et al. (2011) |

Isotope ratios are reported in the conventional δ-notation with respect to V-CDT (Vienna Cañon Diablo Troilite).

Table 5

Morphological features typical of sulfuric acid water table caves classified according to the dominant process.

| | Features also present in thermal hypogenic caves with high CO ₂ concentration from degassing | Typical diagnostic features of sulfuric acid caves |
|--|--|--|
| Hypogenic dominant process | | |
| Flowing corrosive water | | Discharge points with blind termination upstream |
| Standing corrosive pools | Notch with flat roof | |
| Ultra-acidic dripping (mediated by sulfo-oxidant microbial mucoilites) | Ceiling pendant drip hole Drip tubes/wall half tubes | Sulfuric karren Sulfuric cups |
| Condensation–corrosion | Cupola Dome Chimney Wall convection niche Condensation–corrosion channel Megascallops Vent (feeder) Boxwork/weathered walls/hieroglyphs | Corrosion table |
| Corrosion under gypsum cover | | Replacement pockets Massive gypsum deposits |
| Evaporation of moisture | Calcite popcorn (also present in any epigenic cave where strong evaporation takes place) | |

Luisa Sausa, Antonella Scrima, Chiara Tubbiolo, among others. S-stable isotopes of Acqua Fitusa Cave were analyzed at the ETH Zurich by Stefano Bernasconi, while the value for Grotte du Chat was provided by Sandro Galdenzi. Mineralogical analyses of minerals for Acqua Fitusa cave were performed by Ermanno Galli at the University of Modena and Reggio Emilia. Ar/Ar and K/Ar dating was performed by Victor Polyak of the Earth and Planetary Sciences, (University of New Mexico, Albuquerque) and William McIntosh at the New Mexico Bureau of Geology and Mineral Resources (New Mexico Tech, Socorro). The research in Sicily was carried out within the program FFR 2012/2013 (2012-ATE-0136) “Aspetti geomorfologici sul carsismo ipogenico in Sicilia” financed by Palermo University.

References

- Audra, P., 2007. Karst et spéléogénèse épigènes, hypogènes, recherches appliquées et valorisation (Habilitation Thesis) University of Nice Sophia-Antipolis (278 pp.).
- Audra, P., 2008. The sulfuric hypogene speleogenesis: processes, cave pattern, and cave features. *Berl. Höhlenkundliche Ber.* 26, 5–30.
- Audra, P., Mocochain, L., Bigot, J.-Y., Nobécourt, J.-C., 2009a. Hypogene cave patterns. In: Klimchouk, A., Ford, D. (Eds.), *Hypogene Speleogenesis and Karst Hydrogeology of Artesian Basins Special Paper 1*. Ukrainian Institute of Speleology and Karstology, Kiev, pp. 17–22.
- Audra, P., Mocochain, L., Bigot, J.-Y., Nobécourt, J.-C., 2009b. Morphological indicators of speleogenesis: hypogenic speleogenesis. In: Klimchouk, A., Ford, D. (Eds.), *Hypogene Speleogenesis and Karst Hydrogeology of Artesian Basins Special Paper 1*. Ukrainian Institute of Speleology and Karstology, Kiev, pp. 23–32.
- Audra, P., Mocochain, L., Bigot, J.-Y., Nobécourt, J.-C., 2009c. The association between bubble trails and folia: a morphological and sedimentary indicator of hypogenic speleogenesis by degassing, example from Adouste Cave (Provence, France). *Int. J. Speleol.* 38 (2), 93–102.
- Audra, P., Gázquez, F., Rull, F., Bigot, J.-Y., Camus, H., 2015. Hypogene sulfuric acid speleogenesis and rare sulfate minerals in Baume Galinière Cave (Alpes-de-Haute-Provence, France). Record of uplift, correlative cover retreat and valley dissection. *Geomorphology* 247, 25–34.
- Audra, P., Hobléa, F., Bigot, J.-Y., Nobécourt, J.-C., 2007. The role of condensation–corrosion in thermal speleogenesis: study of a hypogenic sulfidic cave in Aix-les-Bains, France. *Acta Carsologica* 36, 185–194.
- Auler, A.S., Smart, P.L., 2003. The influence of bedrock-derived acidity in the development of surface and underground karst evidence from the Precambrian carbonates of semi-arid northeastern Brazil. *Earth Surf. Process. Landf.* 28, 157–168.
- Barton, H., Luiszer, F., 2005. Microbial metabolic structure in a sulfidic cave hot spring: potential mechanisms of biospeleogenesis. *J. Cave Karst Stud.* 67 (1), 28–38.
- Bianchini, G., Gambassini, P., 1973. Le Grotte Dell'acqua Fitusa (Agrigento) I - Gli scavi e l'industria litica. *Riv. Sci. Preistoriche* 28 (1), 1–55.
- Caddeo, G.A., Railsback, R.A.L., De Waele, J., Frau, F., 2015. Stable isotope data as constraints on models for the origin of coralloid and massive speleothems: the interplay of substrate, water supply, degassing, and evaporation. *Sediment. Geol.* 318, 130–141.
- Calaforra, J.M., De Waele, J., 2011. New peculiar cave ceiling forms from Carlsbad Caverns (New Mexico, USA): the zenithal ceiling tube-holes. *Geomorphology* 134, 43–48.
- Catalano, R., Agate, M., Albanese, C., Avellone, G., Basilone, L., Gasparo Morticelli, M., Gugliotta, C., Sulli, A., Valenti, V., Gibilaro, C., Pierini, S., 2013. Walking along a crustal profile across the Sicily fold and thrust belt. AAPG International Conference & Exhibition, 23–26 October 2011, Milan. Post Conference Field Trip 4, 27–29 October 2011, Palermo. *Geological field trips* 5(2.3) (213 pp.).
- Chiesi, M., Forti, P., 1987. Studio morfologico di due nuove cavitá carsiche dell'Iglesiente (Sardegna Sud occidentale). *Ipoantropon* 4, 40–45.
- Collignon, B., 1983. Spéléogénèse hydrothermale dans les Bibans (Atlas Tellien, Algérie). *Karstologia* 2, 45–54.
- Collignon, B., 1990. Les karsts hydrothermaux d'Algérie. 10th International Congress of Speleology Budapest 1989, III, pp. 758–760.
- D'Antoni-Nobécourt, J.-C., Audra, P., Bigot, J.-Y., 2008. La spéléogénèse par corrosion sulfurique: l'exemple de la grotte du Chat (Daluis, Alpes-Maritimes). *Riviera Sci.* 91, 53–72.
- De Waele, J., Forti, P., 2006. A new hypogean karst form: the oxidation vent. *Z. Geomorphol.* 147, 107–127.
- De Waele, J., Forti, P., Naseddu, A., 2013. Speleogenesis of a complex example of an exhumed sulphuric acid karst in Cambrian carbonates (Mount San Giovanni, Sardinia). *Earth Surf. Process. Landf.* <http://dx.doi.org/10.1002/esp.3375>.
- De Waele, J., Galdenzi, S., Madonia, G., Menichetti, M., Parise, M., Piccini, L., Sanna, L., Sauro, F., Tognini, P., Vattano, M., Vigna, B., 2014. A review on hypogene caves in Italy. In: Klimchouk, A., Sasowsky, I., Mylroie, J., Engel, S.A., Engel, A.S. (Eds.), *Hypogene Cave Morphologies*. Karst Waters Institute Special Publication 18, Leesburg, Virginia, pp. 28–30.
- De Waele, J., Plan, L., Audra, P., Rossi, A., Spötl, C., Polyak, V., McIntosh, B., 2009. Kraushöhle (Austria): morphology and mineralogy of an alpine sulfuric acid cave. In: White, W.B. (Ed.), *Proceedings of the 15th International Congress on Speleology, Kerrville, Part 2*, pp. 31–37.
- Dublyansky, V.N., 1980. Hydrothermal karst in Alpine folded belt of southern part of USSR. *Kras Spel.* XII, 18–38.
- Ducluzaux, B., 1994. Karst et thermalisme. 4^e Rencontre d'octobre Pau, Spéléo-club de Paris, pp. 49–52.
- Egemeier, S.J., 1981. Cavern development by thermal waters. *NSS Bull.* 43, 31–51.
- Engel, A.S., Stern, L.A., Bennet, P.C., 2004. Microbial contributions to cave formation: new insights into sulfuric acid speleogenesis. *Geology* 32, 369–372.
- Filippini, M., Jeannin, P.-Y., 2006. Is it possible to predict karstified horizons in tunneling? *Aust. J. Earth Sci.* 99, 24–30.
- Forti, P., 1985. Le mineralizzazioni della grotta di Cala Fetente (Salerno, Campania). *Mondo Sotterraneo* 1985 (1–2), 41–50.
- Forti, P., Galli, E., Rossi, A., 2006. Peculiar minerogenetic cave environments of Mexico: the Cuatro Ciénegas area. *Acta Carsologica* 35 (1), 79–98.
- Forti, P., Menichetti, M., Rossi, A., Hazslinszky, T., Takacsne, B.K., 1989. Speleothems and speleogenesis of the Faggeto Tondo Cave (Umbria, Italy). *Proceedings of the 10th International Congress of Speleology, Budapest*. 1, pp. 74–76.
- Galdenzi, S., 1997. Initial geologic observations in caves bordering the Sibari Plain (Southern Italy). *J. Cave Karst Stud.* 59 (2), 81–86.
- Galdenzi, S., 2001. L'azione morfogenetica delle acque sulfuree nelle Grotte di Frasassi, Acquasanta Terme (Appennino marchigiano-Italia) e di Movile (Dobrogea-Romania). *Le Grotte d'Italia V* (2), 49–61.
- Galdenzi, S., Maruoka, T., 2003. Gypsum deposits in the Frasassi caves, Central Italy. *J. Cave Karst Stud.* 65, 111–125.
- Galdenzi, S., Menichetti, M., 1995. Occurrence of hypogenic caves in a karst region: examples from central Italy. *Environ. Geol.* 26, 39–47.
- Galdenzi, S., Cocchioni, F., Filippini, G., Morichetti, L., Scuri, S., Selvaggio, R., Cocchioni, M., 2000. The sulfidic thermal caves of Acquasanta terme (Central Italy). *J. Cave Karst Stud.* 72 (1), 43–58.
- Gázquez, F., Calaforra, J.-M., Forti, P., De Waele, J., Sanna, L., 2015. The role of condensation in the evolution of dissolutional forms in gypsum caves: study case in the karst of Sorbas (SE Spain). *Geomorphology* 229, 100–111.
- Ginés, J., Fornós, J.J., Ginés, A., Merino, A., Gràcia, F., 2014. Geologic constraints and speleogenesis of Cova des Pas de Vallgornera, a complex coastal cave from Mallorca Island (Western Mediterranean). *Int. J. Speleol.* 43 (2), 105–124.
- Grassa, F., Capasso, G., Favara, R., Inguaggiato, S., 2006. Chemical and isotopic composition of waters and dissolved gases in some thermal springs of Sicily and adjacent volcanic islands, Italy. *Pure Appl. Geophys.* 163, 781–807.
- Hauer, F., 1885. Die Gypsbildungen in der Krausgrotte bei Gams. *Verh. Geol. Reichsanstalt.* 1885, 21–24.
- Hill, C.A., 1987. Geology of Carlsbad cavern and other caves in the Guadalupe Mountains, New Mexico and Texas. *New Mex. Bur. Min. Mineral Resour. Mem.* 117, 1–150.
- Hill, C.A., 1990. Sulfuric acid speleogenesis of Carlsbad Cavern and its relationship to hydrocarbons, Delaware Basin, New Mexico and Texas. *Am. Assoc. Pet. Geol. Bull.* 74, 1685–1694.
- Hose, L.D., Pisarowicz, J.A., 1999. Cueva de Villa Luz, Tabasco, Mexico: reconnaissance study of an active sulfur spring cave and ecosystem. *J. Cave Karst Stud.* 61, 13–21.
- Hose, L.D., Palmer, A.N., Palmer, M.V., Northup, D.E., Boston, P.J., Duchene, H.R., 2000. Microbiology and geochemistry in a hydrogen-sulphide-rich karst environment. *Chem. Geol.* 169, 399–423.
- Jones, D.S., Polerecky, L., Galdenzi, S., Dempsey, B.A., Macalady, J.L., 2015. Fate of sulfide in the Frasassi cave system and implications for sulfuric acid speleogenesis. *Chem. Geol.* 410, 21–27.

- Jones, D.S., Schaperdoth, I., Macalady, J.L., 2014. Metagenomic evidence for sulfide oxidation in extremely acidic cave biofilms. *Geomicrobiol. J.* 31, 194–204.
- Kerckhove, C., Roux, M., 1976. Notice de la Carte Géologique de la France à 1/50 000, 971 Castellane. BRGM, Orléans. 39 pp.
- Kirkland, D.W., 2014. Role of hydrogen sulfide in the formation of cave and karst phenomena in the Guadalupe Mountains and western Delaware Basin, New Mexico and Texas. National Cave and Karst Research Institute, Carlsbad, Special Paper Series 1 (77 pp.).
- Klimchouk, A.B., 2007. Hypogene speleogenesis. Hydrogeological and morphogenetic perspective. National Cave and Karst Research Institute, Carlsbad, Special Paper Series 1 (77 pp.).
- Klimchouk, A.B., 2009. Morphogenesis of hypogenic caves. *Geomorphology* 106, 100–117.
- Kraus, F., 1891. Höhlenbildung durch metamorphismus. *Naturheilkunde* 40, 197–199.
- Lazaridis, G., Melfos, V., Papadopoulou, L., 2011. The first cave occurrence of orpiment (As_2S_3) from the sulfuric acid caves of Aghia Paraskevi (Kassandra Peninsula, N. Greece). *Int. J. Speleol.* 40, 133–139.
- Lombardo, G., Sciumè, A., Sollano, G., Vecchio, E., 2007. La Grotta dell'Acqua Fitusa e l'area della Montagnola nel territorio di San Giovanni Gemini (Ag). *Speleologia Iblea* 12, 125–132.
- Maltsev, V.A., Malishevsky, D.I., 1990. On hydrothermal phases during later stages of the evolution of Cupp Coutunn Cave System, Turkmenia, USSR. *Natl. Speleol. Soc. Bull.* 52, 95–98.
- Martel, E.-A., 1935. Contamination, protection et amélioration des sources thermominérales. *Congr. Int. Min. Métall. Géol. Appl.* 2, 791–798.
- Mayer, A., Wirth, J., 1989. Höhlen und Stollen in Bad Deutsch Altenburg. *Höhlenkundliche Mitt. Wien* 45 (11), 230–234.
- Mecchia, M., 2012. Indizi di speleogenesi ipogenica nelle grotte del Monte Soratte. *Notiziario Speleo Club Roma* 16, 58–69.
- Menichetti, M., 2011. Hypogenic caves in western Umbria (Central Italy). *Acta Carsologica* 40 (1), 129–145.
- Morehouse, D., 1968. Cave development via the sulfuric acid reaction. *NSS Bull.* 30, 1–10.
- Onac, B.P., 1991. New data on some gypsum speleothems in the Vântului (Pădurea Craiului mountains) and Răstoci (Somesan plateau) caves. *Travaux de l'Institut de Spéologie "Emile Racovitza"* 30, pp. 189–193.
- Onac, B.P., Effenberger, H.S., Wynn, J.G., Povară, I., 2013. Rapidcreekite in the sulfuric acid weathering environment of Diana Cave, Romania. *Am. Mineral.* 98, 1302–1309.
- Onac, B.P., Sumrall, J., Tămaș, T., Povară, I., Kearns, J., Dărmiceanu, V., Veres, D., Lascu, C., 2009. The relationship between cave minerals and H_2S -rich thermal waters along the Cerna Valley (SW Romania). *Acta Carsologica* 38 (1), 27–39.
- Onac, B.P., Wynn, J.G., Sumrall, J.B., 2011. Tracing the sources of cave sulfates: a unique case from Cerna Valley, Romania. *Chem. Geol.* 288, 105–114.
- Osborne, R.A.L., 2007. Cathedral Cave, Wellington Cave, New South Wales, Australia. A multiphase, non-fluvial cave. *Earth Surf. Process. Landf.* 32, 2075–2103.
- Palmer, A.N., 2013. Sulfuric acid caves. In: Frumkin, A., Shroder, J. (Eds.), *Treatise on Geomorphology*. Elsevier, pp. 241–257.
- Palmer, A.N., Palmer, M.V., 2000. Hydrochemical interpretation of cave patterns in the Guadalupe Mountains, New Mexico. *J. Cave Karst Stud.* 62, 91–108.
- Palmer, A.N., Palmer, M.V., 2012. Petrographic and isotopic evidence for late-stage processes in sulfuric acid caves of the Guadalupe Mountains, New Mexico, USA. *Int. J. Speleol.* 41 (2), 231–250.
- Pasini, G., 2009. A terminological matter: paragenesis, antigravitative erosion or antigravitational erosion? *Int. J. Speleol.* 38, 129–138.
- Piccini, L., De Waele, J., Galli, E., Polyak, V.J., Bernasconi, S.M., Asmerom, Y., 2015. Sulphuric acid speleogenesis and landscape evolution: Montecchio cave, Albegna river valley (Southern Tuscany, Italy). *Geomorphology* 229, 134–143.
- Plan, L., Spötl, C., Pavuza, R., Dublyansky, Y., 2009. Hypogene caves in Austria. In: Klimchouk, A., Ford, D. (Eds.), *Hypogene Speleogenesis and Karst Hydrogeology of Artesian Basins*. Special Paper, 1. Ukrainian Institute of Speleology and Karstology, Kiev, pp. 121–127.
- Plan, L., Tschegg, C., De Waele, J., Spötl, C., 2012. Corrosion morphology and cave wall alteration in an Alpine sulfuric acid cave (Kraushöhle, Austria). *Geomorphology* 169 (170), 45–54.
- Polyak, V.J., Provencio, P., 2001. By-product materials related to H_2S - H_2SO_4 -influenced speleogenesis of Carlsbad, Lechuguilla, and other caves of the Guadalupe Mountains, New Mexico. *J. Cave Karst Stud.* 63 (1), 23–32.
- Polyak, V.J., DuChene, H.R., Davis, D.G., Palmer, A.N., Palmer, M.V., Asmerom, Y., 2013. Incision history of Glenwood Canyon, Colorado, USA, from the uranium-series analyses of water-table speleothems. *Int. J. Speleol.* 42 (3), 193–202.
- Polyak, V.J., McIntosh, W.C., Provencio, P., Güven, N., 1998. Age and origin of Carlsbad Caverns and related caves from $^{40}Ar/^{39}Ar$ of alunite. *Science* 279, 1919–1922.
- Principi, P., 1931. Fenomeni di idrologia sotterranea nei dintorni di Triponzo (Umbria). *Le Grotte d'Italia* 1 (5), 45–47.
- Puchelt, H., Blum, N., 1989. Geochemische Aspekte der Bildung des Gipsvorkommens der Kraushöhle/Steiermark. *Oberrhein. Geol. Abh.* 35, 87–99.
- Puscas, C.M., Onac, B.P., Effenberger, H.S., Povara, I., 2013. Tamarugite-bearing paragenesis formed by sulfate acid alteration in Diana Cave, Romania. *Eur. J. Mineral.* 25, 479–486.
- Renault, P., 1968. Contribution à l'étude des actions mécaniques et sédimentologiques dans la spéléogénèse. 3e partie: Les facteurs sédimentologiques. *Ann. Spéiol.* 23 (3), 529–596.
- Sanna, L., Saez, F., Simonsen, S.L., Constantin, S., Calaforra, J.M., Forti, P., Lauritzen, S.-E., 2010. Uranium-series dating of gypsum speleothems: methodology and examples. *Int. J. Speleol.* 39 (1), 35–46.
- Sarbu, S.M., Lascu, C., 1997. Condensation corrosion in Movile cave, Romania. *J. Cave Karst Stud.* 59 (3), 99–102.
- Sarbu, S.M., Kane, T.C., Kinkle, B.K., 1996. A chemoautotrophically based cave ecosystem. *Science* 272, 1953–1955.
- Sarbu, S.M., Kinkle, B.K., Vlasceanu, L., Kane, T.C., Popa, R., 1994. Microbiological characterization of a sulfide-rich groundwater ecosystem. *Geomicrobiol. J.* 12, 175–182.
- Schuster, R., Daurer, A., Krenmayr, H.G., Linner, M., Mandl, G., Pestal, G., Reitner, J., 2013. Rocky Austria – Geologie von Österreich kurz und bunt. *Geol. Bundesanstalt, Wien* (80 pp.).
- Socquet, J.-M., 1801. *Analyse des Eaux Thermales d'Aix (en Savoie)*, Département du Mont-Blanc (Analysis of Thermal Waters at Aix, in Savoy, Mont-Blanc Department). Cleaz, Chambéry (240 pp.).
- Spötl, C., Boch, R., Moseley, G., Brandstätter, S., Edwards, R.L., Cheng, H., Mangini, A., Plan, L., 2014. Wann entstanden die tropfsteine in der Kraushöhle bei Gams (Steiermark)? *Höhle* 65, 18–24.
- Stevanović, Z., Iurkiewicz, A., Maran, A., 2009. New insights into karst and caves of north-western Zagros (northern Iraq). *Acta Carsologica* 38 (1), 83–96.
- Szunyogh, G., 1990. Theoretical investigation of the development of spheroidal niches of thermal water origin – second approximation. *Proceedings of the 10th International Congress of Speleology, Budapest*. vol. 3, pp. 766–768.
- Temovski, M., Audra, P., Mihevc, A., Spangenberg, J., Polyak, V., McIntosh, W., Bigot, J.Y., 2013. Hypogenic origin of Provalata Cave, Republic of Macedonia: a distinct case of successive thermal carbonic and sulfuric acid speleogenesis. *Int. J. Speleol.* 42, 235–246.
- Tisato, N., Sauro, F., Bernasconi, S.M., Bruijn, R., De Waele, J., 2012. Hypogenic contribution to speleogenesis in a predominant epigenic karst system: a case study from the Venetian Alps, Italy. *Geomorphology* 151–152, 156–163.
- Vattano, M., Audra, P., Benvenuto, F., Bigot, J.Y., De Waele, J., Galli, E., Madonia, G., Nobécourt, J.C., 2013. Hypogenic caves of Sicily (Southern Italy). In: Filippi, M., Bosak, P. (Eds.), *Proceedings of the 16th International Congress of Speleology, Brno*. vol. 3, pp. 144–149.
- Wessely, G., 1993. Bad Deutsch-Altenburg. In: Goldbrunner, J., Zötl, J. (Eds.), *Die Mineral- und Heilwässer Österreichs*. Springer, pp. 268–272.
- Wynn, J.G., Sumrall, J.B., Onac, B.P., 2010. Sulfur isotopic composition and the source of dissolved sulfur species in thermo-mineral springs of the Cerna Valley, Romania. *Chem. Geol.* 271, 31–43.